Characterization of Sequence-Specific DNA Binding by the Transcription Factor Oct-1†

Thomas Lundbäck,‡,§,|| Ju-Fang Chang,||,⊥,# Kathryn Phillips,⊥ Ben Luisi,⊥ and John E. Ladbury*,‡

Department of Biochemistry and Molecular Biology, University College London, Gower Street, London WC1E 6BT, U.K., and Department of Biochemistry, University of Cambridge, 80 Tennis Court Road, Cambridge CB2 1GA, U.K.

Received February 17, 2000; Revised Manuscript Received April 10, 2000

ABSTRACT: The DNA-binding domain of the Oct-1 transcription factor, POU, recognizes a defined DNA sequence known as the octamer element to regulate the expression of both general and cell-type-specific genes. The two-part DNA-binding domain partially encircles the DNA to recognize the eight base pairs of the octamer element. We have characterized the binding of Oct-1/POU to an octamer element using isothermal titration calorimetry. As found for other cognate protein/DNA complexes, the formation of the Oct-1 POU/DNA complex is associated with a large negative heat capacity change, $\Delta C_{p,obs}$. However, the observed change is much greater than expected by empirical relationships with buried surface area. Supported by data from proteolysis studies on the free and DNA-bound protein, we propose that the discrepancy in heat capacity arises principally from the partial folding of the Oct-1 POU protein upon complex formation. Formation of the Oct-1 POU/DNA complex is strongly dependent on ionic strength, and the detailed quantification of this relationship suggests that six charged contacts are made between the protein and the phosphate groups of the DNA. This agrees with observations from the crystal structure of an Oct-1 POU/DNA complex.

The control of gene expression is fundamental to development and homeostasis of multicellular organisms, in which a large number of different cell types act in a highly coordinated manner. The POU domain family of transcription factors has been identified as important regulators of both developmental and maintenance processes (reviewed in ref *1*). In this study we investigate the sequence-specific DNA binding of one member of this family, the Oct-1 protein. Oct-1 is a ubiquitous transcription factor in mammalian cells and regulates transcription of small nuclear RNA genes and the histone H2B gene (*2*), whose expression is common to most cells. But in addition to regulating these common genes, Oct-1 also regulates cell-specific genes by recruiting other transcription factors or coactivators. For example, Oct-1 interacts with the B-cell-specific protein Bob1 to regulate the transcription of immunoglobulin genes (*3*−*5*). Oct-1 is also known to interact with ligand-inducible hormone receptors, such as the glucocorticoid and the progesterone receptors (*6*).

The biological function of Oct-1 depends on its ability to recognize a defined DNA sequence of eight bases: this target is referred to as the octamer motif (5′-ATGCAAAT-3′ and variations thereof). Oct-1 recognizes the octamer motif through a defined domain, referred to as "POU", because it was first identified in the three transcription factors *P*it-1, *O*ct-1, and *U*NC-86 (*7*). The POU domain has since been identified in a number of other transcription factors (*1*).

The POU domain consists of two conserved and structurally independent subdomains (*8*): the POU-specific (POU_S) domain and the POU-homeo (POU_H) domain (*7*), which contact the DNA on opposite faces of the octamer motif (*9*). The 3.0 Å resolution crystal structure of Oct-1/POU in complex with the H2B promoter shows that both domains use a helix−turn−helix motif to recognize functional groups within the DNA major groove (*9*). The domains are joined by a flexible linker (not seen in the electron density maps), and they are both essential for sequence-specific high-affinity DNA binding (*10*−*12*). The individual domains are capable of binding independently to the octamer motif in the absence of the linker (*13*), and the physical effect of the tethering linker is to ensure an implicit cooperativity in binding (*14*, *15*). Furthermore, despite the lack of intramolecular contacts between POU_S and POU_H in the DNA complex (*9*), biochemical studies demonstrate that the domains influence each other's DNA-binding specificities (*13*, *16*, *17*). It has been suggested that the cooperative binding of the two domains could result from binding-induced changes in the DNA structure (*9*, *13*), and the linker may in fact play an important role in permitting this interplay. The importance of the flexible linker has been much discussed in the literature

† T.L. was supported as a postdoctoral fellow by the Swedish Association for International Cooperation in Higher Education and Research. J.E.L. and B.L. are Wellcome Trust Senior Research Fellows.

* To whom correspondence should be addressed. Tel: (44) 0207 679 7012. Fax: (44) 0207 679 7193. E-mail: j.ladbury@biochem.ucl.ac.uk.

‡ University College London.

§ Present address: Pharmacia and Upjohn, SE-112 87 Stockholm, Sweden.

|| Contributed equally to this work.

⊥ University of Cambridge.

Present address: Department of Biological Chemistry and Molecular Pharmacology, Harvard Medical School, 240 Longwood Ave., Boston, MA 02115.

10.1021/bi000377h CCC: $19.00
Published on Web 05/27/2000

(*1*, *9*, *14*), especially since the linker length is not conserved within the POU domain family. For instance, the various linker lengths might allow the POU_S and POU_H domains to adopt various relative positions and orientations on the DNA and therefore play a key role in the flexibility displayed in the DNA recognition by the POU domain family (*14*). Such flexibility would naturally assist the interaction of this ubiquitous transcription factor with a range of different DNA site arrangements and coactivators and confer onto the protein a certain plasticity in matching DNA targets with varying half-site spacing and polarity.

Detailed studies of the physical basis of DNA binding of individual members of this family should provide some general insights into target recognition by this class of proteins. Here we present a study of the interaction between Oct-1/POU and the octamer motif within the Igκ promoter (*18*) using isothermal titration calorimetry (ITC).[1] The temperature dependence of this interaction has been examined to determine the heat capacity change related to complex formation. ITC data and proteolysis studies suggest that the formation of the protein/DNA complex is accompanied by a significant protein conformational change. The binding has also been studied at a range of different NaCl concentrations to elucidate the role of electrostatic interactions. Combined with detail from the crystal structure of the complex between Oct-1/POU and the octamer motif from the H2B promoter (*9*) and solution structural information from the POU domains (*19*, *20*), our data provide a detailed insight into the nature of this molecular recognition process.

MATERIALS AND METHODS

Protein and DNA Preparation. The expression construct of the Oct-1/POU domain was provided by Dr. Chris Preston, MRC Virology Unit, Glasgow, and was transformed into the *Escherichia coli* BL21 (DE3) strain. The cells were grown and induced with 1 mM isopropyl β-D-thiogalactoside (IPTG). Ammonium sulfate was added to the supernatant after removal of the cell debris to the final concentration of 35%, and the mixture was allowed to equilibrate at 0 °C for 40 min. After the precipitate was removed, the sample was applied to a phenyl−Sepharose column (Pharmacia) and was eluted with a reversed salt gradient. Fractions containing POU protein were dialyzed against a buffer solution containing 10 mM sodium phosphate at pH 7.0 and 20 mM NaCl overnight at 4 °C. Dithiothreitol (DTT) was added to the sample to a final concentration of 5 mM before it was applied to a Mono S column.

Synthetic DNA oligomers (5′-CCAGGGT**ATGCAAAT**-TATTAAGGGC-3′ and its complementary strand) were purified by ion-exchange chromatography using a HPLC Dyanex column. The concentrations of oligonucleotides were determined spectrophotometrically, using extinction coefficients for the individual bases. To correct for hypochromic effects, the absorbance was measured after hydrolysis using phosphodiesterase (Sigma). Complementary strands were mixed in 1:1 stoichiometry and annealed by heating at 85 °C for 5 min and then slowly cooling to room temperature in 100 mM NaCl.

Prior to the ITC experiments (see below) the protein and DNA samples were dialyzed (Spectra/Por molecular porous membrane tubing, MWCO 3500, Spectrum Laboratories, Inc.) overnight in the same beaker to avoid heat signals from mixing of nonequivalent buffers. The following buffers were used: (A) 10 mM sodium phosphate at pH 7.0, 1 mM Na_2-EDTA, 5 mM dithiothreitol (DTT), and 150 mM NaCl; (B) 10 mM Tris at pH 7.0, 1 mM Na_2EDTA, 5 mM DTT, and 150 mM NaCl. After dialysis the samples were filtered through a 0.22 μM filter (MILLEX-GP, Millipore) and the concentrations measured by recording the UV spectrum in 1 cm Hellma quartz cuvettes using a CARY 100 Bio UV−visible spectrophotometer (Varian). The concentrations were calculated using extinction coefficients of $\epsilon_{260nm} = 409.1$ mM^{-1} cm^{-1} and $\epsilon_{280nm} = 24.4$ mM^{-1} cm^{-1} for Igκ and Oct-1/POU, respectively. Samples at a range of different NaCl concentrations were subsequently obtained by adding small amounts of a stock solution containing 10 mM sodium phosphate at pH 7.0, 1 mM Na_2EDTA, 5 mM DTT, and 4.0 M NaCl to both protein and DNA samples in buffer A. The concentrations of these samples were corrected accordingly, and this correction was in no case larger than 8%.

Isothermal Titration Calorimetry. All titrations were carried out using the MCS−ITC instrument from MicroCal Inc., Northampton, MA (see, e.g., ref *21*). Igκ solutions (typically 70−100 μM) were titrated into Oct-1/POU solutions (typically 7−8 μM) using a 250 μL syringe, with each titration consisting of a preliminary 4 μL injection (neglected in the data analysis) followed by 17 subsequent 15 μL injections. Five minutes were left between each injection, and the filter period for data collection was 2 s. The heat associated with each injection was obtained by integrating the area under the resulting peak using the Origin ITC Data Analysis software provided with the instrument. Heats of dilution and injection were measured in control experiments in which the Igκ solutions were titrated into dialysis buffer. These heats were found to be similar to those observed at the end of the DNA/protein titrations, except at 450 mM NaCl where the interaction is further from saturation at the end of the titration. The integrated heats from the DNA/protein experiments were therefore corrected by subtracting the numbers observed toward the end of the titrations, except for the data at 450 mM NaCl where a linear regression line based on the control experiment was subtracted. The data were analyzed to obtain estimates of K_{obs}, n, and ΔH_{cal} and their uncertainties using the "single set of identical sites" model within the Origin software package, except for the data at low NaCl concentration (150 mM) which were also analyzed using a model which takes protein dimerization into account. The protein self-association is described by the mass action law:

$$K_{dimer} = \frac{[PP]}{[P]^2} \qquad f_2 = \frac{2[PP]}{[P]_{tot}} \tag{1}$$

where P denotes the self-associating protein, PP is the dimer, $[P]_{tot}$ is the total protein concentration, K_{dimer} is the dimerization constant, and f_2 is the fraction of protein present as

[1] Abbreviations: DTT, dithiothreitol; Na_2EDTA, ethylenediaminetetraacetic acid disodium salt; IPTG, isopropyl β-D-thiogalactoside; Hepes, *N*-(2-hydroxyethyl)piperazine-*N*′-2-ethanesulfonic acid; Pipes, piperazine-*N*,*N*′-bis(2-ethanesulfonic acid); ITC, isothermal titration calorimetry; K_{obs}, observed binding constant; ΔH_{cal}, calorimetric enthalpy change; n, observed binding stoichiometry; HPLC, high-performance liquid chromatography.

a dimer. The corresponding expression for the DNA binding used by Origin is

$$K_{obs} = \frac{f_1}{(1 - f_1)[D]} \quad (2)$$

where K_{obs} is the observed binding constant for binding of DNA (D) to protein, f_1 is the fraction of each binding site occupied by DNA, and [D] is the concentration of the free, unbound DNA. The mass balances for protein and DNA are

$$[D]_{tot} = [D] + nf_1[P]_{tot}(1 - f_2) \quad (3)$$

$$[P]_{tot} = [P] + 2[PP] + f_1[P]_{tot}(1 - f_2) \quad (4)$$

where n is the number of binding sites on the protein and $[D]_{tot}$ is the total DNA concentration. Note that the dimer fraction is assumed to be unavailable for DNA binding (hence the $1 - f_2$ reduction of $[P]_{tot}$ in the last term in these expressions). These equations are simultaneously solved numerically for a given set of unknown parameters (K_{obs}, K_{dimer}, and n) to obtain physically relevant solutions of f_1 and f_2 using built-in routines within the Mathematica software package (Wolfram Research, Windows NT version 3.0). These parameters can then be used to calculate the expected heat content (Q) in the calorimetrically sensed volume (V_0) following each injection (i) using

$$Q_i = f_{2i}[P]_{tot}\Delta H_{dimer}V_0 + nf_{1i}[P]_{tot}(1 - f_{2i})\Delta H_{cal}V_0 \quad (5)$$

where the subscript i denotes the heat content following injection i, ΔH_{dimer} is the enthalpy of protein dimerization, and ΔH_{cal} is the enthalpy associated with DNA binding. A small correction for displaced volume is made such that the heat released following an injection (ΔQ_i) is given by (as described in the ITC Data Analysis section in the manual provided with the instrument)

$$\Delta Q_i = Q_i + \frac{\delta V_i}{V_0}\left[\frac{Q_i - Q_{i-1}}{2}\right] - Q_{i-1} \quad (6)$$

where δV_i is the injection volume for each data point. The small correction term results from the heat contributed by the small fraction of macromolecular solution that is displaced by the injection. The calculated heats can then be compared with the measured heats for the corresponding injections. The best-fit binding parameters (K_{obs}, ΔH_{cal}, and n or subsets thereof) were determined using nonlinear least-squares fits of eq 6 to the experimental data using routines within Mathematica (K_{dimer} and ΔH_{dimer} were assigned as described below). Errors in the fitted parameters were estimated by fitting of simulated Monte Carlo titrations as described in ref *22*. In short, a random error, which is based on the sensitivity of the instrument (a standard error of 0.6 μcal was assumed), is added to each data point to create a simulated data set. New binding parameters are obtained by fitting the simulated data set, and this procedure is then repeated to produce a set (>10) of binding parameters. The standard deviation of each binding parameter is then calculated from this set.

It is clear that there is a strong correlation between the affinity and enthalpy for protein self-association, i.e., a strong affinity and small magnitude of dimerization enthalpy fit the data equally well as a weak affinity and larger enthalpy, because these combinations both give the characteristic slope observed in the binding isotherms. For this reason one of the parameters must be arbitrarily assigned to a physically relevant number, and then the other parameter is adjusted to produce the characteristic slope. We have chosen to assign $K_{dimer} = 0.17 \times 10^5$ M^{-1} and $\Delta H_{dimer} = 5$ kcal mol^{-1} and keep them fixed during the fits.

In the data collected to determine the ΔC_p we note that the apparent stoichiometry is shifted to lower numbers at the highest temperature (35 °C) as well as for one of the data points at 25 °C. It is not clear what this effect is due to; however, it could result from an incorrect protein concentration determination based on irreversible denaturation prior to performing the ITC experiment.

Surface Area Calculations. The buried surface interface was calculated from the crystal structure of Oct-1/POU in complex with the H2B octamer element using GRASP (*23*). This value represents the area of the DNA, which was covered by the protein, plus the area of the protein covered by the DNA. The nonpolar contribution was obtained by adding the surface areas of all the carbon atoms that are contributing to the interface. The polar interface was calculated by adding the surface areas of all the nitrogen, oxygen, and phosphorus atoms in the interface.

Proteolytic Assays. Samples were dialyzed thoroughly against 10 mM Tris-HCl, pH 8.0, 200 mM NaCl, and 5 mM DTT, at 4 °C with MWCO 3500 membranes. The Oct-1 POU/DNA complex was prepared at a ratio of 1:2 (excess DNA was added to enhance the complex formation) and was incubated at room temperature for 15−30 min before the digestion. Either freshly reconstituted trypsin or chymotrypsin (Boehringer) was then added to the sample solution at a substrate:enzyme ratio (w/w) of 200:1 (about 3−4 μg of each protein was used in each reaction). After incubation at 25 °C, the reaction was stopped by addition of SDS gel sample buffer and heated at 90 °C for 2 min. The products of digestion were separated by a 20% SDS−PAGE gel. Following the gel electrophoresis, proteins were either stained directly with Coomassie blue or transferred by electroelution onto poly(vinylidene difluoride) (PVDF; Bio-Rad) membrane for N-terminal amino acid analysis (service provided by the PNAS facility, University of Cambridge).

RESULTS

Temperature Dependence of Complex Formation. Isothermal titration calorimetry (ITC) was used to study the binding thermodynamics of the interaction between the Oct-1/POU domain and a 25 base pair DNA oligomer based on the Igκ promoter which contains the **ATGCAAAT** octamer motif. A typical titration of Igκ to Oct-1/POU at 25 °C in 150 mM NaCl is shown in Figure 1A. The equivalence point is reached at a molar ratio close to 1 as is more clearly seen in Figure 1B, where the integrated heats are given after correction for the inherent heats of dilution (*21*).

A slight, but reproducible asymmetry is observed in the binding isotherm under these conditions. This asymmetry is also observed in Tris buffer at 150 mM (data not shown).

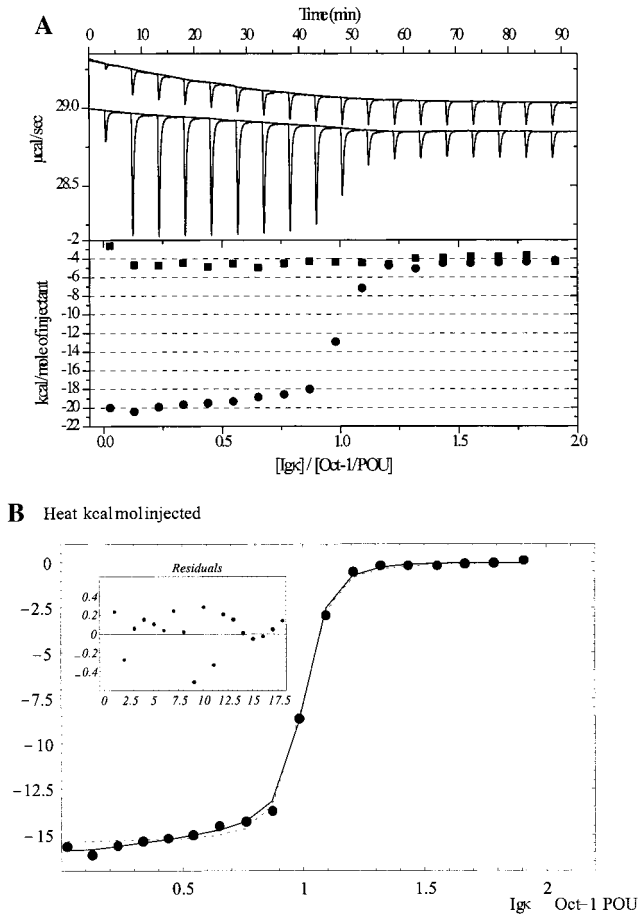

FIGURE 1: (A) Top panel: Raw ITC data from a titration of the Igκ oligomer (77 μM) to a solution containing Oct-1/POU (8.6 μM) at 25.9 °C in 10 mM sodium phosphate, 150 mM NaCl, 1 mM Na_2EDTA, and 5 mM DTT at pH 7.0 (bottom trace). Included is also the raw data from the corresponding control experiment in which Igκ was injected into buffer in the absence of Oct-1/POU (displaced with +0.15 μcal/s for clarity). Both traces are shown with their respective baselines obtained using the ITC Data Analysis package within the Origin software. Bottom panel: Integrated heats normalized with the concentration of Igκ in the syringe from the binding (●) and the control (■) experiment. (B) Illustration of the effect of protein self-association on the binding isotherms. The given heats (●) corrected for heats of dilution were obtained in 10 mM sodium phosphate at pH 7.0, 1 mM Na_2EDTA, 5 mM DTT, and 150 mM NaCl. The solid line represents the best fit to a model involving protein self-association whereas the dotted line is the best fit to a model neglecting protein self-association (see text for details). The inset demonstrates the residuals obtained using the protein self-association model.

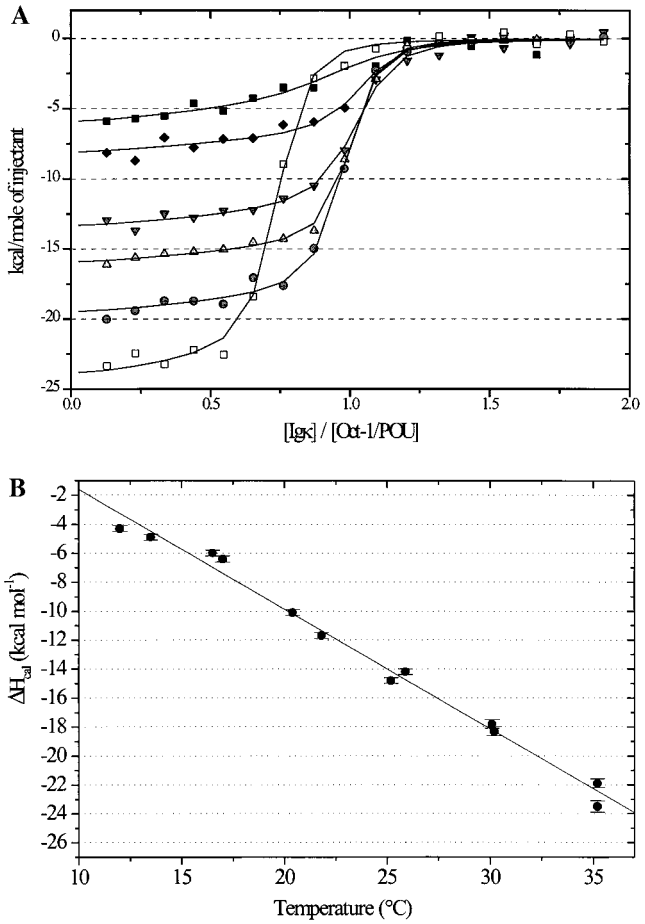

FIGURE 2: (A) Integrated heats normalized with the titrant concentration as a function of the molar ratio of Igκ (77 μM in syringe) to Oct-1/POU (8.6 μM in cell) for a series of isothermal titration calorimetry experiments at different temperatures: 12.0 (■), 17.0 (◆), 21.8 (▼), 25.9 (△), 30.1 (●), and 35.2 °C (□). The given heats are corrected for heats of dilution. The titrations were carried out in 10 mM sodium phosphate at pH 7.0, 150 mM NaCl, 1 mM Na_2EDTA, and 5 mM DTT. The solid lines represent best fits to theoretical binding isotherms as described in the text. (B) Observed binding enthalpy for the interaction of Igκ with Oct-1/POU as a function of temperature (●). The solid line represents a linear regression analysis of the data with a slope of -0.83 ± 0.03 and a correlation coefficient of $r = 0.99$.

This type of effect is observed, for example, when the titrand is weakly self-associating. Oct-1/POU dimers have been observed at micromolar concentrations in chemical cross-linking experiments in solutions at low salt concentration [50 mM NaCl (*24*)]. This protein dimerization has been found to be significantly reduced with increased salt concentration (*24*). Since the ITC experiments herein reported are carried out at a total protein concentration of approximately 7−8 μM, the protein could be self-associated to some extent. Unfortunately, a significant lowering of the protein concentration to avoid this potential problem is not possible due to limitations in the ITC instrument sensitivity. We fitted our data using the single set of noninteracting identical sites model, but to investigate the impact of dimerization on the best-fit parameters, we additionally evaluated our data obtained at 150 mM NaCl using a model which accounted for weak self-association (see Materials and Methods). The effect of using the more complex model for the data at 150 mM NaCl is demonstrated in Figure 1B, where the fits to the different models are compared. As expected when introducing additional parameters, the fit is improved, but it is important to emphasize that this results in relatively moderate alterations of the reported thermodynamic quantities for sequence-specific DNA binding by Oct-1/POU (Table 1). The use of the protein self-association model results in a marginally less exothermic enthalpy (+1.5 kcal mol^{-1}) for DNA binding and a slightly stronger affinity compared to the simpler model. Regardless of these considerations the binding is too strong under these conditions to allow an accurate determination of the binding affinity (see, e.g., refs *22* and *25*), so the numbers in Table 1 should be considered low estimations of the binding affinity. The numbers translate to a maximal free energy change ($\Delta G°_{obs}$) of -10.6 ± 0.2 kcal mol^{-1}, demonstrating that the DNA binding is completely dominated by an enthalpic driving

Table 1: Temperature Dependence of Sequence-Specific DNA Binding of Oct-1/POU[a]

temp (°C)	$K_{obs} \times 10^{-6}$ (M^{-1})	N	ΔH_{cal} (kcal mol^{-1})	$K_{dimer}{}^{b} \times 10^{-5}$ (M^{-1})	$\Delta H_{dimer}{}^{b}$ (kcal mol^{-1})
12.0	5.6 ± 1.6 (3.6 ± 1.6)	0.93 ± 0.02 (0.86 ± 0.04)	−4.3 ± 0.2 (−5.9 ± 0.4)	0.17	5.0
13.5	11 ± 4 (5.8 ± 2.5)	1.00 ± 0.02 (0.95 ± 0.04)	−4.9 ± 0.2 (−6.4 ± 0.4)	0.17	5.0
16.5	37 ± 10 (18 ± 8)	0.99 ± 0.01 (0.96 ± 0.02)	−6.0 ± 0.2 (−7.4 ± 0.3)	0.17	5.0
17.0	26 ± 12 (14 ± 6)	1.00 ± 0.01 (0.97 ± 0.02)	−6.4 ± 0.2 (−7.8 ± 0.3)	0.17	5.0
20.4	30 ± 8 (20 ± 7)	1.01 ± 0.01 (0.99 ± 0.02)	−10.1 ± 0.2 (−11.4 ± 0.3)	0.17	5.0
21.8	27 ± 8 (19 ± 5)	0.98 ± 0.01 (0.96 ± 0.01)	−11.7 ± 0.2 (−13.0 ± 0.2)	0.17	5.0
25.2	60 ± 16 (47 ± 8)	0.76 ± 0.01 (0.75 ± 0.01)	−14.8 ± 0.2 (−16.3 ± 0.2)	0.17	5.0
25.9	58 ± 13 (44 ± 8)	0.96 ± 0.01 (0.94 ± 0.01)	−14.2 ± 0.2 (−15.4 ± 0.2)	0.17	5.0
30.1	43 ± 10 (32 ± 7)	0.93 ± 0.01 (0.92 ± 0.01)	−17.8 ± 0.3 (−19.1 ± 0.3)	0.17	5.0
30.2	25 ± 5 (22 ± 5)	0.97 ± 0.01 (0.96 ± 0.01)	−18.3 ± 0.3 (−19.5 ± 0.3)	0.17	5.0
35.2	39 ± 9 (32 ± 6)	0.72 ± 0.01 (0.72 ± 0.01)	−21.9 ± 0.3 (−23.4 ± 0.3)	0.17	5.0
35.2	37 ± 8 (33 ± 10)	0.74 ± 0.01 (0.73 ± 0.01)	−23.5 ± 0.4 (−24.9 ± 0.5)	0.17	5.0

[a] Best-fit parameters and their uncertainties were obtained using the single set of noninteracting identical sites model within the Origin ITC Data Analysis software (numbers given within parentheses) and alternatively with a model involving protein self-association (see the text for details). The buffer solution was 10 mM sodium phosphate at pH 7.0, 1 mM Na_2EDTA, 5 mM DTT, and the indicated NaCl concentration. [b] Arbitrary choice of thermodynamic parameters for protein self-association. See the text for details.

Table 2: Salt Dependence of the Sequence-Specific DNA Binding of Oct-1/POU at 25 °C[a]

[NaCl]	$K_{obs} \times 10^{-6}$ (M^{-1})	N	ΔH_{cal} (kcal mol^{-1})	$K_{dimer}{}^{b} \times 10^{-5}$ (M^{-1})	$\Delta H_{dimer}{}^{b}$ (kcal mol^{-1})
150	82 ± 75 (71 ± 18)	1.05 ± 0.01 (1.04 ± 0.01)	−12.6 ± 0.2 (−13.8 ± 0.2)	0.17	5.0
	107 ± 27 (69 ± 15)	1.04 ± 0.01 (1.03 ± 0.01)	−12.6 ± 0.2 (−13.7 ± 0.2)	0.17	5.0
	79 ± 37 (56 ± 17)[c]	0.97 ± 0.01 (0.96 ± 0.01)[c]	−9.8 ± 0.2(−10.7 ± 0.2)[c]	0.17[c]	5.0[c]
200	79 ± 36	1.03 ± 0.02	−11.2 ± 0.3		
	48 ± 14	1.03 ± 0.01	−11.4 ± 0.2		
250	20 ± 10	1.00 ± 0.03	−11.0 ± 0.5		
	26 ± 6	1.04 ± 0.01	−11 ± 0.2		
350	3.6 ± 1.2	1.02 ± 0.03	−10.1 ± 0.5		
	3.2 ± 0.8	1.03 ± 0.03	−10.0 ± 0.4		
450	0.74 ± 0.26	0.86 ± 0.08	−8.1 ± 1.0		
	1.3 ± 0.6	1.18 ± 0.07	−7.4 ± 0.7		

[a] Best-fit parameters and their uncertainties were obtained using the single set of noninteracting identical sites model within the Origin ITC Data Analysis software, except for the data at 150 mM NaCl which were also analyzed using a model involving protein self-association (see the text for details). In this case the numbers observed using the simpler model are given within parentheses. The buffer solution was 10 mM sodium phosphate at pH 7.0, 1 mM Na_2EDTA, 5 mM DTT, and the indicated NaCl concentration. [b] Arbitrary choice of thermodynamic parameters for protein self-association. See the text for details. [c] In 10 mM Tris at pH 7.0, 1 mM Na_2EDTA, 5 mM DTT, and the indicated NaCl concentration.

force at 25 °C. We have recently used ITC to study the interaction between Oct-1/POU and a number of similar octamer targets, which differed in only a single base pair or contained strategically chosen base pair modifications (*26*). The protein binding interactions to all of the chosen sites were exothermic at room temperature, in qualitative agreement with the polar nature of this interaction.

To obtain the apparent change in heat capacity ($\Delta C_{p,obs}$) of complex formation, the enthalpy of binding was measured at a range of temperatures between 12 and 35.2 °C. The integrated heats from the titrations at these temperatures are shown in Figure 2A, where the solid lines through the data points represent the best fits to the binding model which considers weak self-association. The use of this model was motivated by the presence of the asymmetry in the binding isotherm at all of these temperatures (as described above and shown in Figure 2A). The best-fit parameters are summarized in Table 1 along with those that were obtained using the single set of noninteracting identical sites model. It should be pointed out that the asymmetry observed is similar at all temperatures and, as a consequence, the enthalpies are systematically but moderately less exothermic using the protein self-association model (by approximately 1.5 kcal mol^{-1}).

ΔH_{cal} for sequence-specific DNA binding is exothermic at all temperatures, and it depends strongly on temperature. This is further illustrated in Figure 2B, where ΔH_{cal} is plotted as a function of temperature. The solid line represents a linear regression of the data with a slope of $\Delta C_{p,obs} = -0.83 \pm 0.03$ kcal mol^{-1} K^{-1} with a correlation coefficient of $r = 0.99$. It should be stressed that the $\Delta C_{p,obs}$ value determined using the best-fit parameters from the simpler model, in which protein dimerization is neglected, is very similar to that quoted above. The linearity of the $\Delta C_{p,obs}$ plot indicates that there are no other temperature-dependent equilibria occurring on complex formation. Protonation effects associated with complex formation have been shown to contribute to $\Delta C_{p,obs}$. Data obtained in Tris rather than phosphate buffer under similar conditions at 25 °C are accompanied by a somewhat lower ΔH_{cal} ($\Delta\Delta H_{cal} \approx 3$ kcal mol^{-1}; Table 2). However, the respective heats of ionization for these buffers are very different [$\Delta\Delta H_{ion} \approx 10$ kcal mol^{-1} (*27*)], indicating that only a fraction of a proton is taken up at these conditions. Thus there is likely to be only a small contribution to the $\Delta C_{p,obs}$ from protonation effects. The $\Delta C_{p,obs}$ is unlikely to arise from DNA duplex melting as UV melting curves and differential scanning calorimetry experiments confirmed that the DNA was stable in the temperature range in which the heat capacity change was determined [melting temperature was 65−70 °C depending on the sample concentration (data not shown)]. Although Oct-1/POU showed significant precipitation during the thermal unfolding experiment, this only occurred above 45 °C when at concentrations approximating those used in ITC. This precipitation was likely to result from

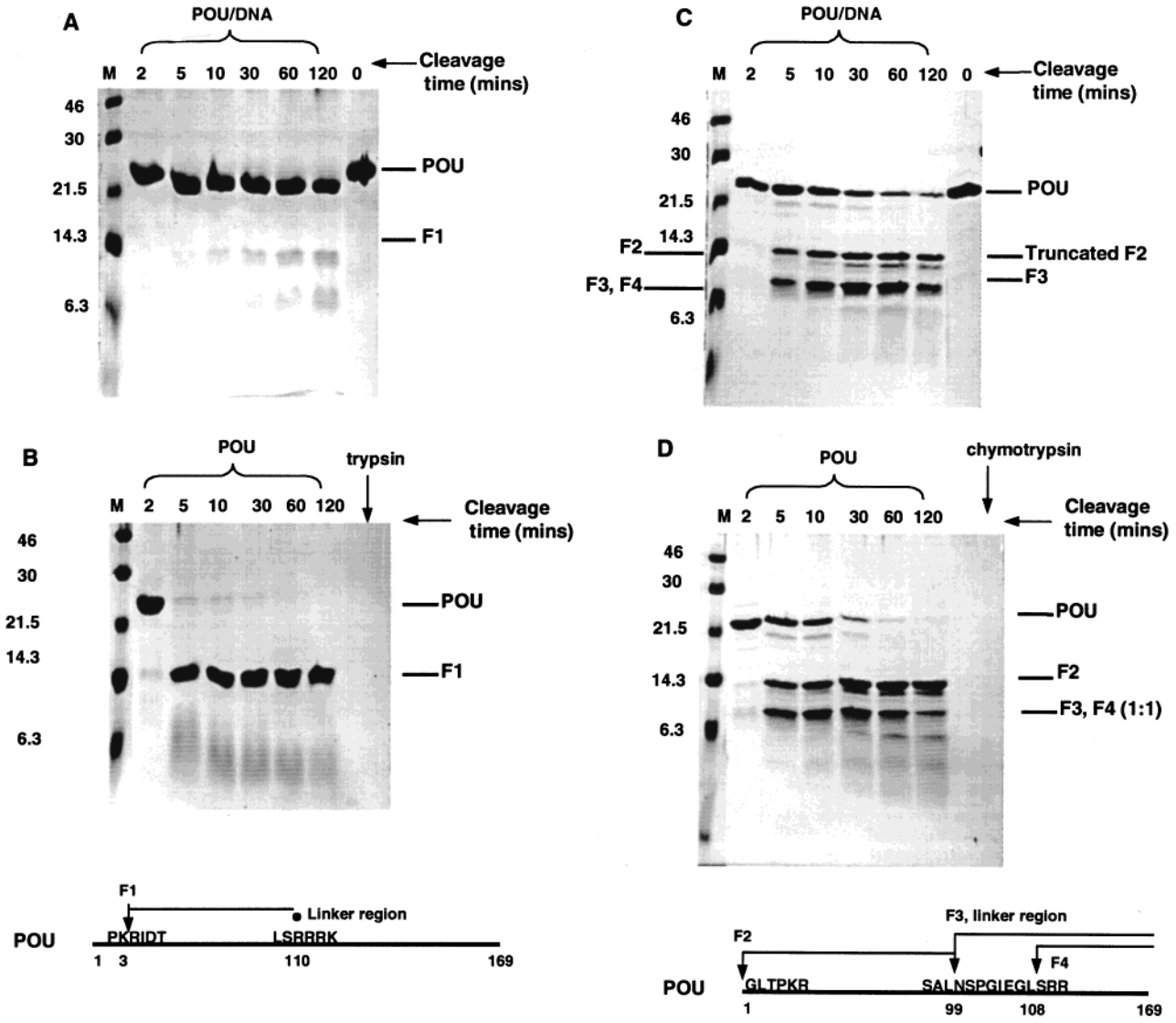

FIGURE 3: Proteolytic cleavage experiments. (A) Trypsin cleavage of the Oct-1 POU/DNA complex. (B) Trypsin cleavage of free Oct-1 POU. A summary of the digest products is shown in the bottom panel (below B), where the numbers indicate the positions of amino acids; the arrows show the sites of digestion which are the N-termini of the identified fragments. The length of the fragments is estimated from the apparent weight of the gel and the potential cleavage sites shown in Figure 4. (C) Chymotrypsin cleavage of the Oct-1 POU/DNA complex. (D) Chymotrypsin cleavage of the free Oct-1 POU complex. A summary of the digest products is shown in the bottom panel, where the numbers indicate the positions of amino acids; the arrows show the sites of digestion which are the N-termini of the identified fragments. The length of the fragments is estimated from the apparent weight of the gel and the potential cleavage sites shown in Figure 4. Time points in the protease digestion reaction have been run in consecutive lanes. Lanes outside of the time course have been moved adjacent to the reaction for clarity.

the aggregation of unfolded Oct-1/POU protein at this temperature.

POU_H Is Proteolytically Cleaved in the Absence of DNA. The protein/DNA complex and the free protein were digested with either trypsin (Figure 3A,B) or chymotrypsin (Figure 3C,D) to probe for relative structural stability. Limited proteolysis of the Oct-1 POU domain with trypsin produced a stable band with an apparent molecular mass of 14 kDa (fragment F1; Figure 3). N-Terminal sequence analysis showed that this product corresponded to a single species that is a C-terminally truncated POU-specific (POU_S) domain fragment starting from the third residue, Arg^3, as predicted from the digest map (Figure 4). The C-terminus of POU was apparently completely degraded. We do not observe any other stable product that could possibly correspond to the POU-homeo (POU_H) domain, even in the early stages of digestion.

Chymotrypsin digestion gave complementary results. Two distinct bands were produced by the digestion (Figure 3D). N-Terminal sequencing showed that the upper, 14 kDa fragment (F2) represents the truncated POU_S domain, while the second band at 7 kDa is a 1:1 mixture of two fragments which contain the POU_H domain and originate from two cleavage sites in the flexible linker region (Asn^{99} and Ser^{108}), generating fragments F3 and F4. With further incubation, the 7 kDa fragment was degraded, while the 14 kDa one remained intact. This is consistent with the observations from the trypsin digest, which indicated that the POU_H domain is more sensitive to proteolysis than the POU_S domain.

POU_H Is Protected from Proteolysis in the Protein/DNA Complex. Formation of the protein/DNA complex conferred protection against trypsin digestion (Figure 3B). In contrast to the free protein, where the digestion was almost complete after 5 min, the DNA complex was resistant to prolonged

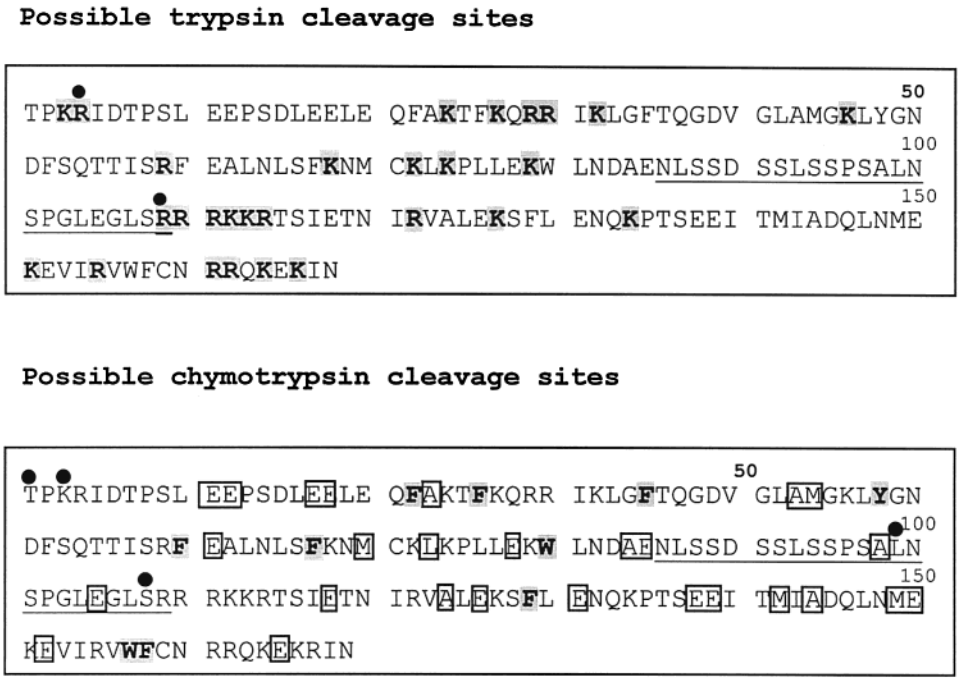

FIGURE 4: Potential trypsin and chymotrypsin cleavage sites in the Oct-1 POU domain. Trypsin is a serine endopeptidase specifically hydrolyzing proteins and peptides at the carboxylic side of the basic amino acids Arg and Lys (shown in bold font and lightly shaded). Chymotrypsin is also a serine endopeptidase that specifically hydrolyzes peptide bonds at the carboxylic side of Tyr, Phe, and Trp residues (bold and lightly undershaded). Met, Ala, and Glu are cleaved at a lower rate (boxed letters). Filled dots indicate the N-terminus of the identified cleavage products. The linker region of the Oct-1 POU domain is underlined.

trypsin exposure (greater than 2 h). It seems likely that the trypsin sites in the free POU domain became less accessible in the DNA complex. Although the C-terminus of the linker region contains a short segment of trypsin sites (RRRKKR; amino acids 109−114), the crystal structure shows that it is partly surrounded by both DNA and the POU_H domain (*9*), which may explain its relative resistance to proteolysis.

The presence of DNA protected the POU protein against chymotrypsin digestion, although the digestion pattern was similar for the free and bound proteins (Figure 3C,D), as shown by N-terminal sequencing (Figure 3D; fragments F2, F3, and F4). The POU_H/POU_S linker contains several potential chymotrypsin recognition sites (Figure 4), and the crystal structure shows that the linker region is largely flexible. As expected, digestion yielded two fragments which correspond to the individual subdomains. At the end of the digestion course, an appreciable amount of intact DNA-bound POU remained, while in its free state, POU was almost completely degraded within 1 h (Figure 3C). These observations are consistent with the linker becoming less conformationally flexible in the complex.

Salt Dependence of Complex Formation. Figure 5 includes ITC data obtained at a range of different NaCl concentrations from 150 to 450 mM. The solid lines represent best fits to the data using a model with a single set of independent binding sites, except for the data at 150 mM NaCl that was analyzed as described previously. The best-fit parameters are summarized in Table 2. Whereas the observed binding stoichiometry (n) is close to 1 at all conditions, the observed binding constant (K_{obs}) as well as the calorimetric enthalpy (ΔH_{cal}) is strongly dependent on the NaCl concentration.

Panels B and C of Figure 5 demonstrate the dependency of the logarithm of K_{obs} and of ΔH_{cal}, respectively, on the logarithm of total Na^+ concentration (which includes Na from NaCl, NaH_2PO_4, and NaOH). The significant reduction in K_{obs} with increased NaCl concentration is consistent with sequence-specific DNA binding (*28*, *29*) and represents the release of counterions from the highly charged DNA molecule. The plot is linear at salt concentrations above 200 mM NaCl, with a correlation coefficient of $r = 0.99$ and the slope of this line, $SK_{obs} = -5.4 \pm 0.3$. This number translates to the formation of six ion pairs in the protein/DNA complex (*28*, *29*), in good agreement with structural data on a related complex where six phosphates are within 3.0 Å of positively charged amino acid residues (*9*). The DNA in the crystal structure, from the H2B promoter, has the same octamer sequence as the Igκ promoter studied here but differs in the regions flanking the octamer site. Included in Figure 5B are three data points reported in the literature for binding to the octamer site at a slightly lower concentration of monovalent cations [≈115 mM (*12*, *24*, *30*)], and they fall reasonably close to the regression line. An affinity of a similar magnitude has also been observed at very low salt concentrations (*31*). The ΔH_{cal} plot (Figure 5C) also demonstrates a strong dependence on salt concentration. A linear regression results in a correlation coefficient of 0.95, and the equation that approximates the salt dependence is $\Delta H_{cal} = 9.7 \log [Na^+] - 5.1$. The physical interpretation of this observation is discussed in the next section.

DISCUSSION

We have used isothermal titration calorimetry to determine the thermodynamic characteristics of binding of the Oct-1/POU and a 25 base pair oligonucleotide corresponding to the Igκ promoter. On the basis of previously reported observations at low salt, we fit our data at 150 mM using a simple model, which assumes only two interacting compo-

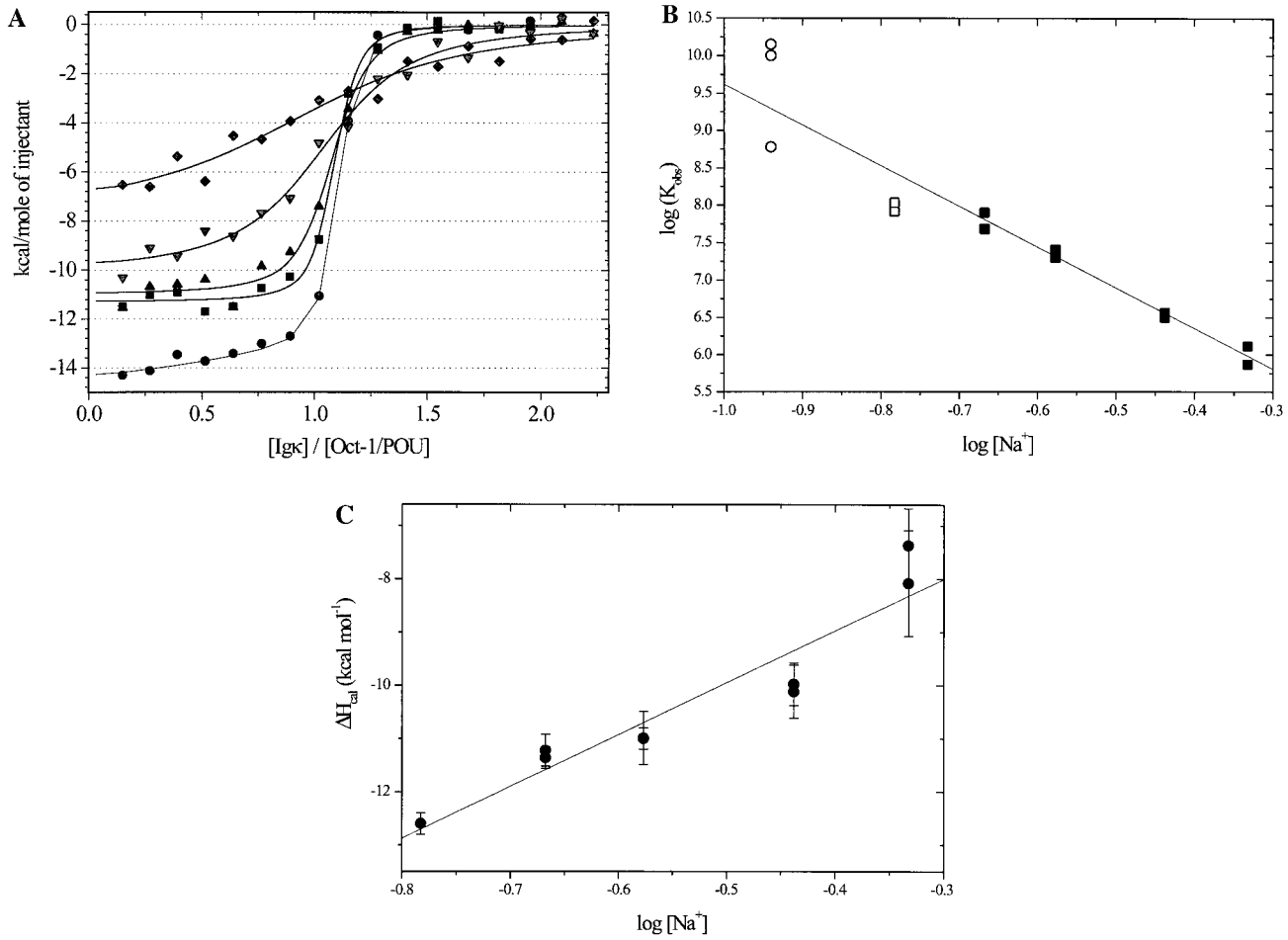

FIGURE 5: (A) Integrated heats normalized with the titrant concentration as a function of the molar ratio of Igκ to Oct-1/POU for a series of isothermal titration calorimetry experiments at different salt concentrations. The given heats are corrected for heats of dilution and are the average of two independent titrations. The titrations were carried out in 10 mM sodium phosphate at pH 7.0, 1 mM Na_2EDTA, 5 mM DTT, and 150 (●), 200 (■), 250 (▲), 350 (▼), or 450 (◆) mM NaCl. The solid lines represent best fits to theoretical binding isotherms for the single set of identical sites model within the Origin software package, except for the data at 150 mM NaCl which was analyzed using a model that considers protein self-association (see the text for details). (B) Logarithm of the observed binding constant for binding of Igκ to Oct-1/POU as a function of the logarithm of total Na^+ concentration (■). The solid line represents a linear regression analysis of the data, neglecting the data points at 150 mM NaCl (highlighted using □). The slope of the line is $SK_{obs} = -5.4 \pm 0.3$ with a correlation coefficient of $r = 0.99$. Included in the figure (open circles) are also previously published estimations of K_{obs} for binding to octamer sites from various promoter regions using gel mobility shift assays (*12*, *24*, *30*). (C) Observed binding enthalpy for the interaction of Igκ with Oct-1/POU as a function of the logarithm of total Na^+ concentration (●). The solid line represents a linear regression analysis of the data, with a slope of 9.7 ± 1.1, an intercept of -5.1 ± 0.7, and a correlation coefficient of $r = 0.95$.

nents, and a more complex model which includes protein dimerization (in which the dimer does not bind DNA). Application of these two distinct models actually results in only moderate differences in best-fit parameters for sequence-specific DNA binding. It is, of course, possible that self-association might occur also at higher salt concentrations. However, we believe that this is not the case for the following reasons. (1) The published data on the dimerization of Oct-1/POU demonstrate that this interaction is strongly salt dependent, with micromolar binding being observed at 50 mM NaCl. Dissociation of the dimer is observed in affinity chromatography experiments at 150 mM NaCl, and no binding is observed at 300 mM NaCl and above (*24*). (2) The asymmetry in the binding isotherms is not observed at the higher salt concentrations. (3) The SK_{obs} plot (Figure 3B) is linear at salt concentrations above 150 mM, as might be expected for the highly charged interaction between protein and DNA (*28*, *29*).

The thermodynamic study presented here demonstrates that the formation of an interface between Oct1/POU and a cognate DNA sequence involves a significant perturbation of the system. The formation of highly complementary protein/DNA complexes is generally accompanied by large negative changes in heat capacity (*32*, *33*). Several studies using calorimetry have demonstrated this ΔC_p effect in protein/DNA interactions (e.g., refs *34*−*39*). In most reported protein/DNA interactions a large surface area of the interacting molecules is secluded from bulk solvent. Empirical relationships have been developed which relate the magnitude of ΔC_p to changes in solvent-exposed surface area of the interacting macromolecules (see, e.g., refs *40* and *41*). However, whereas the hydration of small model compounds as well as protein folding processes appears to be reasonably well described by these relationships, large discrepancies are often seen for protein/DNA interactions. Mechanisms such as DNA-binding-induced protein folding (*33*, *42*), linked protonation and ion binding events (*43*, *44*), and "stiffening" of soft vibrational modes at the interface particularly from entrapped water molecules (*35*, *45*) provide potential explanations for the discrepancies.

No structural data on the complex of Oct-1/POU with the Igκ promoter to assess the correlation between ΔC_p and surface area have been reported. We have adopted the published structure of the complex between the protein and the H2B promoter (*9*) as a model for this calculation. The oligonucleotide in this structure differs from the Igκ sequence only in the region flanking the octamer element, and thus a high level of structural homology is expected. Using the published structure, we could calculate the burial of surface area on complex formation. The calculations are based on the assumption that the interaction between Oct-1/POU and Igκ can be modeled by a docking between two rigid macromolecules, both of which are taken from the structure of the complex. The change in polar surface area (ΔA_p) upon complexation was found to be 2236 Å^2, whereas the corresponding number for nonpolar surfaces (ΔA_{np}) was 1018 Å^2. These numbers illustrate the highly polar nature of the interaction surface, and using the equation suggested (*41*), we obtain $\Delta C_{p,calc} = -12.0 \pm 2.0$ cal mol^{-1} K^{-1}. Thus there is a large discrepancy between the calculated ΔC_p on complex formation and that determined experimentally (-830 ± 30 cal mol^{-1} K^{-1}).

Here we propose that the concomitant folding of protein on binding to the DNA is likely to be responsible, at least in part, for the discrepancy in the ΔC_p values. On the basis of previously reported data (*40*), the observed discrepancy would correspond to the complete burial of approximately 26 additional amino acid side chains on complex formation. From published solution structural data on both POU domains (*19*, *20*), the POU-homeo domain of Oct-1 is partially disordered when it is in isolation; however, on forming a complex with the DNA, part of the recognition helix appears to become ordered. The ordering of the structure reported in the NMR spectroscopic data involves approximately 10 amino acids at the C-terminus of the domain (*20*). The burial of these residues would not provide a sufficient contribution to ΔC_p on forming the complex to account for the discrepancy; thus the experimentally determined value is not fully accounted for by the folding described by the homeo domain (see above). This would suggest that either additional conformational changes could occur. It is possible that a contribution to burial of additional surface area comes from other parts of the protein and/or DNA not observed in the solution structural studies. For example, the flexible linker between the two Oct-1/POU domains could be at least partially buried on complex formation. Although this part of the protein is not clearly defined in the crystal structure, it is possible that some interactions with the DNA remove amino acid surface from bulk solvent. Furthermore, conformational changes within the POU_S domain cannot be ruled out, even though structural detail (*19*) and proteolytic cleavage experiments suggest that this domain is likely to be well folded.

Proteolytic cleavage experiments enhance the hypothesis that a significant structural change occurs on binding. Both trypsin and chymotrypsin proteolytic cleavage patterns show that the POU_S domain is significantly more protected than the POU_H domain. This has been previously observed for the POU_S and POU_H domains of Oct-2/POU protein, which shares a high sequence identity with Oct-1/POU (*8*). Binding of the protein to DNA results in limited degradation even after 2 h incubation with trypsin. This is indicative of the cleavage sites being buried in the complex either in the protein/DNA interface or as the result of protein folding. These data are consistent with the POU_H domain not being completely folded in its unbound state, but becoming more structured, which incurs a significant burial of the polypeptide chain on binding DNA.

Importantly, the lack of curvature in the ΔC_p plot in the temperature range studied (Figure 2B) suggests that the protein folding event has to be temperature independent; i.e., the same amount of structure is involved in refolding. Thus the conformational change effected on binding is constant at all temperatures studied, and there is no resulting temperature dependence of ΔC_p. This folding event is likely, therefore, to represent a specific induced-fit mechanism rather than the DNA merely stabilizing protein structure.

It is not clear where the observed dependence of the enthalpy on the salt concentration emanates from (Figure 5C). Again, there are a number of possible sources. The release of counterions from DNA is generally expected to be purely entropic in origin (see, e.g., refs *27* and *28*); however, some recent studies have suggested that this is not always the case (*43*, *44*). In these studies the enthalpic contribution is attributed to specific ion binding and/or release from either protein or oligonucleotide. A further enthalpic component which could be reflected in the salt dependence could be derived from the weak protonation event that is observed in this study. This would be based on a DNA-binding-induced increase of the pK_a of a group in the proximity of DNA phosphates, which is likely to be salt dependent. Any of these events would add an enthalpic component to the salt-dependent free energy, and additional experiments are required to establish the nature of this effect. However, it is worth pointing out that the heat capacity plot is devoid of any significant curvature, indicating that the event is strongly coupled to the formation of the protein/DNA complex. As such, it might also have an impact on the magnitude of the observed heat capacity change.

The interaction of Oct-1 with an oligonucleotide corresponding to the Igκ promoter results in a significant structural rearrangement on binding. Our data reveal a large discrepancy in the experimentally determined and the empirically derived ΔC_p values. On the basis of previous structural evidence, this is likely to be accrued in a protein folding event that occurs on binding DNA. The lack of curvature in the plot of ΔH against temperature suggests that this folding is consistent over the large temperature range studied. This might be an important characteristic of induced-fit mechanisms frequently seen in protein/DNA interactions.

REFERENCES

1. Ryan, A. K., and Rosenfeld, M. G. (1997) *Genes Dev. 11*, 1207−1225.
2. Herr, W. (1992) in *Transcriptional regulation* (McKnight, S., and Yamamoto, K., Eds.) Cold Spring Harbor Laboratory Press, Cold Spring Harbor, NY.
3. Luo, Y., and Roeder, R. G. (1995) *Mol. Cell. Biol. 15*, 4115−4124.
4. Gstaiger, M., Georgiev, O., van Leeuwen, H., van der Vliet, P., and Schaffner, W. (1996) *EMBO J. 15*, 2781−2790.
5. Strubin, M., Newell, J. W., and Matthias, P. (1995) *Cell 80*, 497−506.
6. Brüggemeier, U., Kalff, M., Franke, S., Scheidereit, C., and Beato, M. (1991) *Cell 64*, 565−572.

7. Herr, W., Sturm, R. A., Clerc, R. G., Corcoran, L. M., Baltimore, D., Sharp, P. A., Ingraham, H. A., Rosenfeld, M. G., Finney, M., Ruvkun, G., and Horvitz, H. R. (1988) *Genes Dev. 2*, 1513−1516.
8. Botfield, M. C., Jansco, A., and Weiss, M. A. (1992) *Biochemistry 31*, 5841−5848.
9. Klemm, J. D., Rould, M. A., Aurora, R., Herr, W., and Pabo C. O. (1994) *Cell 77*, 21−32.
10. Sturm, R. A., and Herr, W. (1988) *Nature 336*, 601−604.
11. Ingraham, H. A., Flynn, S. E., Voss, J. W., Albert, V. R., Kapiloff, M. S., Wilson, L., and Rosenfeld, M. G. (1990) *Cell 61*, 1021−1033.
12. Verrijzer, C. P., Kal, A. J., and van der Vliet, P. C. (1990) *Genes Dev. 4*, 1964−1974.
13. Klemm, J. D., and Pabo, C. O. (1996) *Genes Dev. 10*, 27−36.
14. Herr, W., and Cleary, M. A. (1995) *Genes Dev. 9*, 1679−1693.
15. Perutz, M. (1990) *Mechanisms of cooperativity and allosteric regulation in proteins*, Cambridge University Press, New York.
16. Aurora, R., and Herr, W. (1992) *Mol. Cell. Biol. 12*, 455−467.
17. Verrijzer, C. P., Alkema, M. J., van Weperen, W. W., van Leeuwen, H. C., Strating, M. J. J., and van der Vliet, P. C. (1992a) *EMBO J. 11*, 4993−5003.
18. Falkner, F. G., and Zachau, H. G. (1984) *Nature 310*, 71−74.
19. Cox, M., Dekker, N., Boelens, R., Verrijzer, C. P., van der Vliet, P. C., and Kaptein, R. (1993) *Biochemistry 32*, 6032−6040.
20. Cox, M., van Tilborg, P. J., de Laat, W., Boelens, R., van Leeuwen, H. C., van der Vliet, P. C., and Kaptein, R. (1995) *J. Biomol. NMR 6*, 23−32.
21. Ladbury, J. E. (1995) *Structure 3*, 635−639.
22. El Harrous, M., and Parody-Morreale, A. (1997) *Anal. Biochem. 254*, 96−108.
23. Nicholls, A., Sharp, K. A., and Honig, B. (1991) *Proteins: Struct., Funct., Genet. 11*, 281−296.
24. Verrijzer, C. P., van Oosterhout, J. A. W. M., and van der Vliet, P. C. (1992b) *Mol. Cell. Biol. 12*, 542−551.
25. Wiseman, T., Williston, S., Brandts, J. F., and Lin, L.-N. (1989) *Anal. Biochem. 179*, 131−137.
26. Chang, J.-F., Phillips, K., Lundbäck, T., Gstaiger, M., Ladbury, J. E., and Luisi, B. (1999) *J. Mol. Biol. 288*, 941−952.
27. Izatt, R. M., and Christensen, J. J. (1976) in *CRC Handbook of Biochemistry and Molecular Biology: Physical and Chemical Data* (Fasman, G. D., Ed.) 3rd ed., Vol. I, pp 151−269, CRC Press Inc., Cleveland, OH.
28. Record, M. T., Jr., Anderson, C. F., and Lohman, T. M. (1978) *Q. Rev. Biophys. 2*, 103−178.
29. Record, M. T., Jr., Ha, J.-H., and Fisher, M. A. (1991) *Methods Enzymol. 208*, 291−343.
30. Nakshatri, H., Nakshatri, P., and Currie, R. A. (1995) *J. Biol. Chem. 270*, 19613−19623.
31. van Leeuwen, H. C., Strating, M. J., Cox, M., Kaptein, R., and van der Vliet, P. C. (1995) *Nucleic Acids Res. 23*, 3189−3197.
32. Whitson, P. A., Olson, J. S., and Matthews, K. S. (1986) *Biochemistry 25*, 3852−3858.
33. Ha, J.-H., Spolar, R., and Record, M. T. (1989) *J. Mol. Biol. 209*, 801−816.
34. Takeda, Y., Ross, P. D., and Mudd, C. P. (1992) *Proc. Natl. Acad. Sci. U.S.A.* 8180−8184.
35. Ladbury, J. E., Wright, J. G., Sturtevant, J. M., and Sigler, P. B. (1994) *J. Mol. Biol. 238*, 669−681.
36. Hyre, D. E., and Spicer, L. D. (1995) *Biochemistry 34*, 3212−3221.
37. Merabet, E., and Ackers, G. K. (1995) *Biochemistry 34*, 8554−8563.
38. Lundbäck, T., and Härd, T. (1996) *Proc. Natl. Acad. Sci. U.S.A. 93*, 4754−4759.
39. O'Brien, R., DeDecker, B., Fleming, K. G., Sigler, P. B., and Ladbury, J. E. (1998) *J. Mol. Biol. 279*, 117−125.
40. Murphy, K. P., and Freire, E. (1992) *Adv. Protein Chem. 43*, 313−361.
41. Spolar, R. S., Livingstone, J. R., and Record, M. T., Jr. (1992) *Biochemistry 31*, 3947−3955.
42. Spolar, R. S., and Record, M. T. (1994) *Science 263*, 777−784.
43. Lohman, T. M., Overman, L. B., Ferrari, M. E., and Kozlov, A. G. (1996) *Biochemistry 35*, 5272−5279.
44. Kozlov, A. G., and Lohman, T. M. (1998) *J. Mol. Biol. 278*, 999−1014.
45. Morton, C. J., and Ladbury, J. E. (1996) *Protein Sci. 5*, 2115−2118.

BI000377H